Atomic layer deposition of W on nanoporous carbon aerogels

J. W. Elam,[a] J. A. Libera, M. J. Pellin, A. V. Zinovev, J. P. Greene, and J. A. Nolen
Argonne National Laboratory, Argonne, Illinois 60439

(Received 1 March 2006; accepted 12 June 2006; published online 4 August 2006)

In this study, the authors demonstrate the ability to apply precise, conformal W coatings onto all surfaces of nanoporous carbon aerogels using atomic layer deposition (ALD). The resulting material has a filamentous structure in which the W completely encapsulates the carbon aerogel strands. The material mass increases nonlinearly with W coating, achieving a tenfold increase following ten ALD cycles. The aerogel surface area increases by nearly a factor of 2 after ten W ALD cycles. This conformal metal coating of extremely high aspect ratio nanoporous materials by ALD represents a unique route to forming metal functionalized high surface area materials. © *2006 American Institute of Physics*. [DOI: 10.1063/1.2245216]

Carbon aerogels are a class of nanoporous aerogel solids with high porosity and low density.[1–9] Because of their high conductivity, carbon aerogels are often used electrochemically[10,11] and as supercapacitors.[10,12] The desire to produce stable, high surface area catalytic electrodes has generated significant interest in incorporating metal catalytic sites onto the inner surfaces of such materials.[11,13–16] In addition, the infiltration of carbon aerogels with high Z metals is an innovative route to prepare spallation neutron targets for the production of radioactive beams at facilities such as ISOLDE/CERN or ATLAS.[17–19] Spallation targets must be highly dense to efficiently stop an energetic ion beam, but also must possess interior channels to allow rapid diffusion of the radionuclides to the accelerator source. W-coated aerogels possess both properties since the initial high surface area allows the coated monoliths to achieve significant mass with coatings of only a few monolayers.

Atomic layer deposition (ALD) is a thin film growth method utilizing alternating, self-limiting exposures to reactive gases to deposit material in a monolayer-by-monolayer fashion.[20] ALD has been used previously to apply precise metal-oxide coatings onto nanoporous solids[21,22] including silica aerogels.[23] In addition, ALD has been used to deposit metal particles on the inner surfaces of anodic aluminum oxide (AAO).[24,25] However, until now there has been no report describing the conformal coating of extremely high aspect ratio nanoporous solids by ALD metal films. This may be due in part to the difficult challenge of nucleating metal growth on nonmetallic surfaces.[20,26] W ALD using alternating exposures to disilane (Si_2H_6) and tungsten hexafluoride (WF_6) was chosen for this study both because of its high Z and because it is among the best studied ALD metal systems.[26–31] One concern is the potential for non-self-limiting growth resulting from the thermal decomposition of Si_2H_6.[28]

Carbon aerogel monoliths with a density of 0.082 g/cm^3 and a surface area of 214 m^2/g were obtained from the Stanford Research Institute. Scanning electron microscope (SEM) images reveal that the carbon aerogels are comprised of an interconnected network of solid carbon filaments with diameters of ~10 nm separated by gaps of ~10 nm. The monoliths were cut into slabs with dimensions of $1 \times 50 \times 10$ mm^3 and subsequently coated by ALD using a custom apparatus[32] operated in a quasistatic mode.[21] To promote W nucleation,[29] the carbon aerogels were first coated with a thin (~0.2 nm) ALD Al_2O_3 layer using two cycles of trimethyl aluminum (TMA) and H_2O with reactant exposures of 5 Torr for 10 min at a temperature of 200 °C separated by 5 min purges in flowing nitrogen. Subsequently, W ALD was performed at 200 °C using alternating exposures to 5 Torr Si_2H_6 for 10 min and 10 Torr WF_6 for 10 min separated by 5 min purges in flowing nitrogen. To minimize oxidation of the W, the carbon aerogels were cooled slowly to 40 °C under flowing nitrogen prior to exposing the samples to air. Failure to perform this cooling step resulted in violent, immediate burning upon air exposure. In addition to the carbon aerogels, Si(100) wafers and AAO membranes with a pore diameter of $d=40$ nm and a thickness of $L=70$ μm were coated under the same conditions. The Si(100) wafers facilitate measurement of the W coating thickness using ellipsometry, while the well-defined AAO pore geometry allows evaluation of the ALD W conformality in extremely high aspect ratios ($L/d=1750$).

Figure 1(a) shows a plan view SEM image of the AAO membrane following two Al_2O_3 ALD cycles for nucleation followed by ten ALD cycles and reveals a W film comprised of nanocrystals with a lateral dimension of ~2 nm (arrow) on the surface of the hexagonally arranged nanopore array. Energy dispersive x-ray analysis (EDAX) measurements from the middle of the cleaved AAO membrane yield 8 at. % W and this value is consistent with a W film thickness of ~7 nm given the AAO geometry. Figure 1(c) shows an EDAX W line scan along the cleaved cross section of the AAO membrane shown in Fig. 1(b) and demonstrates uniform W infiltration throughout the AAO. The background noise level for these data is ~8 counts. Figure 2(a) shows the W thickness measurements versus number of W ALD cycles on the ALD Al_2O_3-coated Si(100) wafers. Following an induction period of two to three cycles, the W grows linearly at 7.2 Å/cycle. This induction period may reflect a lower reactivity and nucleation density of W sites on the initial Al_2O_3 surface compared to W.

Figure 2(b) presents the change in relative mass of the carbon aerogel versus number of W ALD cycles. The mass following W coating was determined using a Denver Instruments APX-100 digital analytical balance with 0.1 mg sen-

[a]Electronic mail: jelam@anl.gov

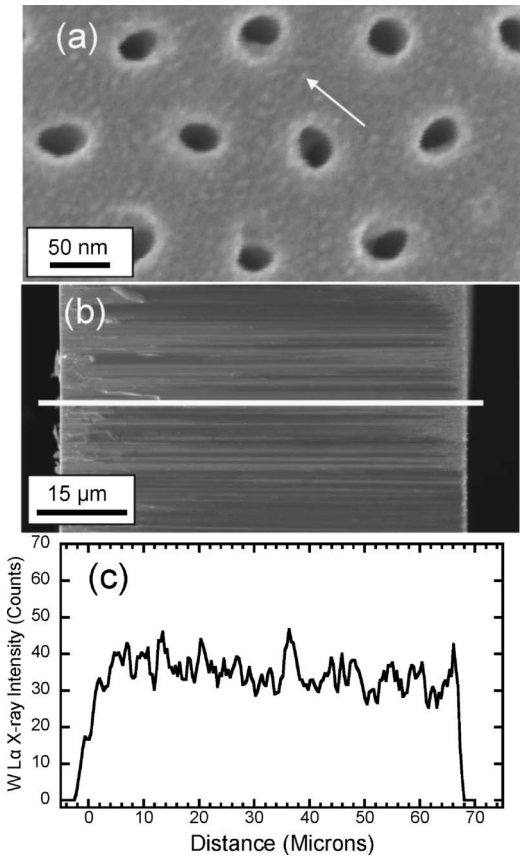

FIG. 1. Plan view (a) and cross-sectional (b) SEM images of anodic aluminum oxide membrane following ten cycles of W ALD. The white arrow indicates W nanocrystal. W EDAX line scan (c) taken from the middle of the cleaved membrane along the white line in (b).

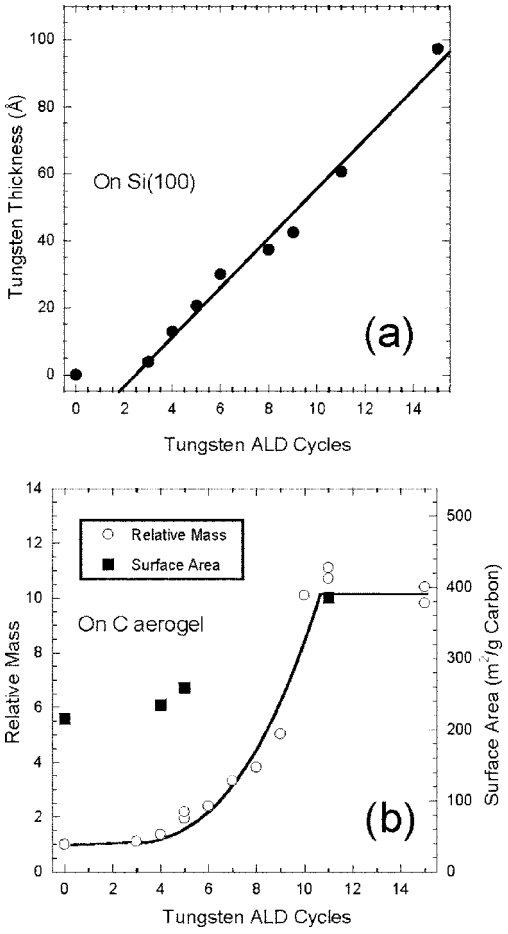

FIG. 2. W thickness vs number of ALD W cycles on planar Si(100) surface (a). Relative mass and surface area of W-coated carbon aerogel vs number of ALD W cycles (b).

sitivity and this quantity was divided by the initial carbon aerogel mass (~0.5 g), yielding the relative mass change with an estimated uncertainty of ±10%. In agreement with Fig. 2(a), the carbon aerogel mass does not begin increasing until three to four ALD cycles. Following this induction period, the W mass increases quadratically with the number of cycles in contrast to the linear W growth on planar Si(100). This behavior can be understood as a linear increase in surface area resulting from the linear ALD W growth on the outer surfaces of the aerogel filaments. To support this explanation, the surface area of the carbon aerogels was measured by nitrogen adsorption using the Brunauer-Emmett-Teller (BET) method.[33] Figure 2(b) demonstrates that the surface area (expressed as m^2 per gram of carbon) increased by nearly a factor of 2 over the ten W ALD cycles. The growth of W on the carbon aerogel abruptly terminated following ten ALD cycles, suggesting closure of ~10 nm voids between the filaments on the outside of the aerogel preventing further ALD growth on the interior.

Figure 3 displays SEM and EDAX elemental mapping images of a cleaved cross section of the carbon aerogel following 15 W ALD cycles. The outer surface of the monolith is on the right side of each image, while the left side of each image is more than halfway through the 1 mm monolith. The uniformity of the W EDAX map demonstrates complete infiltration of the ALD W into the interior of the aerogel. Figure 4 supports this conclusion. This figure displays transmission electron microscope (TEM) images recorded from interior fragments of the carbon aerogel after three and seven

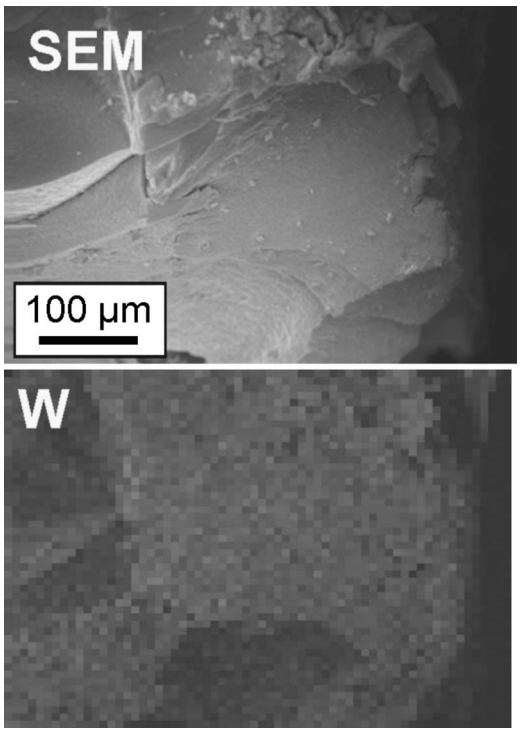

FIG. 3. SEM image and EDAX W elemental mapping image of cleaved cross section of carbon aerogel following 15 cycles of ALD W.

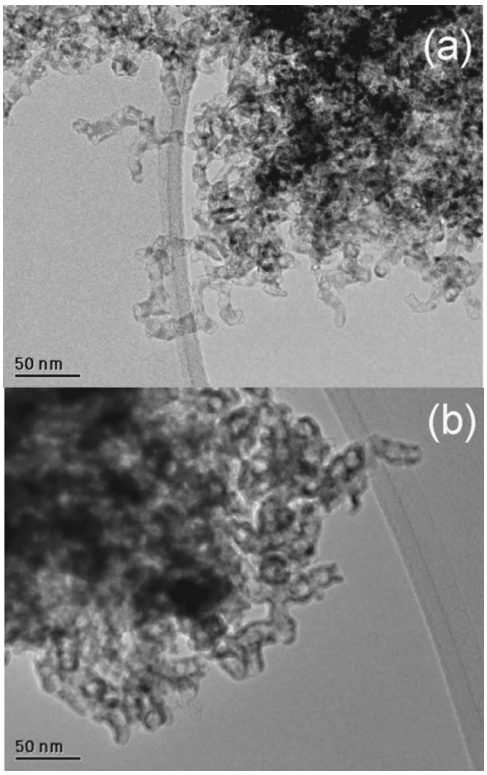

FIG. 4. TEM images of carbon aerogel following three (a) and seven (b) cycles of W ALD.

ALD cycles [Figs. 4(a) and 4(b), respectively]. Because two to four ALD cycles are necessary to nucleate the W ALD, the first figure shows essentially no increase in the aerogel filament diameter over the uncoated carbon aerogel. However, the increased filament diameter in Fig. 4(b) is consistent with the approximately threefold mass increase following seven W ALD cycles shown in Fig. 2(b). The small pores visible in Fig. 4(a) support our theory that closure of the voids between the filaments terminates the W growth after ten ALD cycles. Additional TEM and BET pore size distribution measurements could evaluate this idea. X-ray photoelectron spectroscopy measurements of the W-coated carbon aerogels show a combination of metallic and oxidized W peaks consistent with a thin native oxide on the W surface that forms upon air exposure.

In conclusion, we have demonstrated the metallization of nanoporous AAO and carbon aerogels using ALD. The broad range of known ALD metal chemistries makes this an attractive and versatile synthetic technique for the metallization of nanoporous solids. These materials have application ranging from catalysis and electrocatalysis to spallation targets for radionuclide beam generation.

The work at Argonne is supported by the U.S. Department of Energy, BES-Materials Sciences under Contract No. W-31-109-ENG-38. Electron microscopy was performed at the Electron Microscopy Center at Argonne National Laboratory. The authors would like to express gratitude to Lennox Iton for allowing use of his BET apparatus and to Hao Wang for supplying the AAO membranes.

[1] S. Berthon-Fabry, D. Langohr, P. Achard, D. Charrier, D. Djurado, and F. Ehrburger-Dolle, J. Non-Cryst. Solids **350**, 136 (2004).
[2] V. Bock, O. Nilsson, J. Blumm, and J. Fricke, J. Non-Cryst. Solids **185**, 233 (1995).
[3] J. Gross and J. Fricke, J. Non-Cryst. Solids **186**, 301 (1995).
[4] T. Horikawa, J. I. Hayashi, and K. Muroyama, Carbon **42**, 169 (2004).
[5] F. M. Kong, J. D. LeMay, S. S. Hulsey, C. T. Alviso, and R. W. Pekala, J. Mater. Res. **8**, 3100 (1993).
[6] W.-C. Li, A.-H. Lu, and S.-C. Guo, J. Colloid Interface Sci. **254**, 153 (2002).
[7] G. Reichenauer, A. Emmerling, J. Fricke, and R. W. Pekala, J. Non-Cryst. Solids **225**, 210 (1998).
[8] D. Wu, R. Fu, Z. Sun, and Z. Yu, J. Non-Cryst. Solids **351**, 915 (2005).
[9] R. Zhang, Y. Lue, Q. Meng, L. Zhan, G. Wu, K. Li, and L. Ling, J. Porous Mater. **10**, 57 (2003).
[10] S. J. Kim, S. W. Hwang, and S. H. Hyun, J. Mater. Sci. **40**, 725 (2005).
[11] N. Yoshizawa, H. Hatori, Y. Soneda, Y. Hanzawa, K. Kaneko, and M. S. Dresselhaus, J. Non-Cryst. Solids **330**, 99 (2003).
[12] S.-W. Hwang and S.-H. Hyun, J. Non-Cryst. Solids **347**, 238 (2004).
[13] T. F. Baumann, G. A. Fox, J. H. Satcher, Jr., N. Yoshizawa, R. Fu, and M. S. Dresselhaus, Langmuir **18**, 7073 (2002).
[14] R. Fu, T. F. Baumann, S. Cronin, G. Dresselhaus, M. S. Dresselhaus, and J. H. Satcher, Jr., Langmuir **21**, 2647 (2005).
[15] F. J. Maldonado-Hodar, C. Moreno-Castilla, and A. F. Perez-Cadenas, Appl. Catal., B **54**, 217 (2004).
[16] C. Moreno-Castilla, F. J. Maldonado-Hodar, and A. F. Perez-Cadenas, Langmuir **19**, 5650 (2003).
[17] S. Lukic, F. Gevaert, A. Kelic, M. V. Ricciardi, K. H. Schmidt, and O. Yordanov, Los Alamos National Laboratory, Report No. nucl-ex/0601031, 2006 (unpublished).
[18] T. Fritioff, J. Cederkaell, L. Weissman, C. J. Barton, K. A. Connell, D. Duniec, O. Kester, T. Lamy, T. Nilsson, P. Jardin, P. Sortais, and G. Transtroemer, Nucl. Instrum. Methods Phys. Res. A **556**, 31 (2006).
[19] U. Koster, T. Behrens, C. Clausen, P. Delahaye, V. N. Fedoseyev, L. M. Fraile, R. Gernhuuser, T. J. Giles, A. Ionan, T. Kroll, H. Mach, B. Marsh, M. Seliverstov, T. Sieber, E. Siesling, E. Tengborn, F. Wenander, and J. Van de Walle, CERN-EP/2005–033, 2005 (unpublished).
[20] M. Ritala and M. Leskelä, *Handbook of Thin Film Materials* edited by H. S. Nalwa (Academic, San Diego, CA, 2001), Vol. 1, p. 103.
[21] J. Elam, D. Routkevitch, P. Mardilovich, and S. George, Chem. Mater. **15**, 3507 (2003).
[22] M. J. Pellin, P. C. Stair, G. Xiong, J. W. Elam, J. Birell, L. Curtiss, S. M. George, C. Y. Han, L. Iton, H. Kung, M. Kung, and H.-H. Wang, Catal. Lett. **102**, 127 (2005).
[23] S. O. Kucheyev, J. Biener, Y. M. Wang, T. F. Baumann, K. J. Wu, T. van Buuren, A. V. Hamza, J. H. Satcher, Jr., J. W. Elam, and M. J. Pellin, Appl. Phys. Lett. **86**, 083108 (2005).
[24] A. Johansson, J. Lu, J. O. Carlsson, and M. Boman, J. Appl. Phys. **96**, 5189 (2004).
[25] A. Johansson, T. Torndahl, L. M. Ottosson, M. Boman, and J. O. Carlsson, Mater. Sci. Eng., C **23**, 823 (2003).
[26] J. W. Elam, C. E. Nelson, R. K. Grubbs, and S. M. George, Thin Solid Films **386**, 41 (2001).
[27] J. W. Klaus, S. Ferro, and S. M. George, Thin Solid Films **360**, 145 (2000).
[28] J. W. Elam, C. E. Nelson, R. K. Grubbs, and S. M. George, Surf. Sci. **479**, 121 (2001).
[29] R. K. Grubbs, C. E. Nelson, N. J. Steinmetz, and S. M. George, Thin Solid Films **467**, 16 (2004).
[30] Z. A. Sechrist, F. H. Fabreguette, O. Heintz, T. M. Phung, D. C. Johnson, and S. M. George, Chem. Mater. **17**, 3475 (2005).
[31] F. H. Fabreguette, Z. A. Sechrist, J. W. Elam, and S. M. George, Thin Solid Films **488**, 103 (2005).
[32] J. Elam, M. Groner, and S. George, Rev. Sci. Instrum. **73**, 2981 (2002).
[33] S. Lowell and J. E. Shields, *Powder Surface Area and Porosity* (Chapman and Hall, New York, 1991), p. 14.